The Cryosphere Discuss., https://doi.org/10.5194/tc-2019-82
Manuscript under review for journal The Cryosphere
Discussion started: 2 May 2019

The Cryosphere Discussions
Open Access
EGU

Detecting of Cave Floor Ice Dynamics based on Selective Cloud-to-Cloud Approach

Jozef Šupinský[1], Ján Kaňuk[1], Zdenko Hochmuth[1], Michal Gallay[1]

[1] Institute of Geography, Pavol Jozef Šafárik University, Košice, Jesenná 5, 040 01, Slovakia

Correspondence to: Jozef Šupinský (jozef.supinsky@upjs.sk)

Abstract. Ice caves can be considered as an indicator of the long-term changes in the landscape. Dynamics in ice volume in the caves are common throughout the year, but the inter-seasonal comparison of ice dynamics indicates a change in the hydrological-climatic regime of the landscape. However, evaluating cave ice volume changes is a challenging task that requires continuous monitoring based on detailed mapping. Nowadays, laser scanning technology is used for cryomorphology mapping to record a status of the ice at an ultra-high resolution. In order to evaluate the dynamics of cave ice, it is necessary to place individual measurements in an unified coordinate system. In the presented paper, we propose a selective cloud-to-cloud approach that addresses the issue of registration of single scan missions into unified coordinate system. We present the results of the ice dynamics monitoring in the Silická ľadnica cave situated in the Slovak Karst, which started in summer of 2016. Based on the results we can conclude that the change in ice volume during the year is continuous and we can observe repeated processes of degradation and ice formation in the cave. Presented analysis of the inter-seasonal dynamics of the ice volume demonstrates that there has been a significant decrement of ice in the monitored period.

1 Introduction

Ice caves are considered as the most dynamic types of caves in terms of morphology and speleoclimate changes which results from numerous processes acting inside the cave but also in its immediate exterior surroundings (Perșoiu and Lauritzen, 2018). Cave ice originates and accumulates mainly as a result of water freezing and to a lesser extent of snow densification and diagenesis (Perșoiu, 2018). The morphology of ice is more dynamic than the surface of carbonate speleothems for higher plasticity and sensitiveness to cave micro-climate. The dynamics of the cave glaciers and ice accumulations was studied by combining various sources of data and methods. Assessment of photographic material has been the most widely used for monitoring the extent of the ice and its change (Fuhrmann, 2007). The other methods comprise markers distributed and attached on the ice floor and/or cave walls (Pflitsch et al., 2016), geodetic surveying (Gašinec et al., 2014), absolute dating (Luetscher et al., 2007) and drilling (May et al., 2011). Complex monitoring programs of detecting cave ice accumulations dynamics has been built in caves sporadically (Kern and Perșoiu, 2013). Complex programs for monitoring the cave ice dynamics were introduced in few cases (Perșoiu and Pazdur, 2011; Kern and Thomas, 2014).

Quantifying the changes of ice accumulations over a certain period in high spatial resolution can improve understanding of the cave ice formation including factors affecting the accumulation or loss of ice. The challenge is in defining the method by which cryomorphological topography could be recorded fast, repeatedly and reliably. In the last decade, terrestrial laser scanning (TLS) provided opportunity to map the challenging environment of the caves in an unprecedented level of detail (Gallay et al., 2015). TLS is an active remote sensing technique allowing for contactless sampling of the 3-D point positions on the surface of the scene surrounding the scanner with a millimetre accuracy and precision (Vosselman and Maas, 2010). The point density controls the spatial resolution depending on the distance of the surface to the scanner and technical settings of the scanner. It typically ranges between few millimetres at 10-metre distance. Point clouds containing millions of the 3D measurements generated from consecutive scanner positions can be merged and unified in the process of mutual registration based on a common feature in the overlapping areas. Cave surface can be modelled from the point cloud as a 3-D polygonal mesh or a 2.5 raster surface, which was demonstrated in Gallay et al. (2016). Applications of TLS in non-glaciated caves are diverse comprising the field of geomorphology (Cosso et al., 2014; Silvestre et al., 2014; Idrees and Pradhan, 2016; Fabbri et al., 2017, De Waele et al., 2018), light conditions (Hoffmeister et al., 2014), archeology (Gonzalez-Aguilera et al., 2009, Rüther et al., 2009; Lerma et al., 2010) to increase awareness and tourism (Buchroithner et al., 2011; Buchroithner et al., 2012) etc. However, use of TLS in ice caves is more challenging for the slippery surface, harsh climate and reflectance of the ice absorbing much of the laser energy emitted by the scanner (Kamintzis et al., 2018). Examples of using TLS in glaciers and ice (Bauer et al., 2003; Avian and Bauer, 2006; Gašinec et al., 2012; Gabbud et al., 2015; Fischer et al., 2016; Xu et al., 2018) and snow depth change (Jörg et al., 2006; Kaasalainen et al., 2008; Prokop, 2008; Deems et al., 2013). Gómez-Lende and Sánchez-Fernández (2018) demonstrate potential of (TLS) technology in the mapping of ice accumulations in the caves. Using TLS, it is possible to repeat measurements and generate time-series of cryomorphological topographies easily. Avian et al. (2018) also addressed this issue with terrestrial laser scanning (TLS) in the ice cave, but some questions remain open.

In order to assessment of the ice accumulations changes based on TLS point clouds, adjustment and re-locating single measurements (point clouds) into an uniform coordinate system is required. Barnhart and Crosby (2013) used a global coordinate system for TLS point clouds based on the ground control points (GCPs) acquired via Global Navigation Satellite Systems (GNSS). The disadvantage of this approach is that it is also necessary to scan parts of the cave exterior where GNSS signal is strong enough to obtain the GCPs. Traditionally, a system of stabilized GCPs located in a cave and acquired based on geodetic methods such as tachymetry is used (Gašinec et al., 2014). The placement of the GCPs on the cave floor is not possible in many caves due to the changing ice accumulations. On other side, placing of the GCPs on the wall of cave at a sufficient height is very demanding and risky. In addition, within long-term monitoring program the position of the GCPs is uncertain due to frost, water and erosion, that is, the GCPs could be shifted.

The presented paper builds on the published experience and further develops of the methodology of detecting changes in ice accumulations using TLS. We described a framework of registration procedure based on selective cloud-to-cloud approach and generating time series database. The novelty is also in the procedure for deriving complex 3D cave model from point clouds using mesh model. Based on presented methodology, we identified and quantified cave floor ice changes in the high

The Cryosphere Discuss., https://doi.org/10.5194/tc-2019-82
Manuscript under review for journal The Cryosphere
Discussion started: 2 May 2019

resolution and assessed dynamics of cryomorphological topography using parameters such as profiles, area and volume as well.

Proposed approach was demonstrated in the case study of the Silická ľadnica ice cave situated in the south margin of the Western Carpathians in Slovakia, Central Europe.

2 Area of Interest

The Silická ľadnica cave is one of the oldest well-explored ice cave in Slovakia (Bella and Zelinka, 2018). The cave (Fig. 1) is located in the southwest of eastern Slovakia on the Silická planina (Silica plateau) in the Slovak Karst. The cave is unique for preserving the ice accumulations on the cave floor at the lowest altitude in the world being in moderate climate zone. Droppa (1962) estimated that ice accumulations are in the cave about 2000 years.

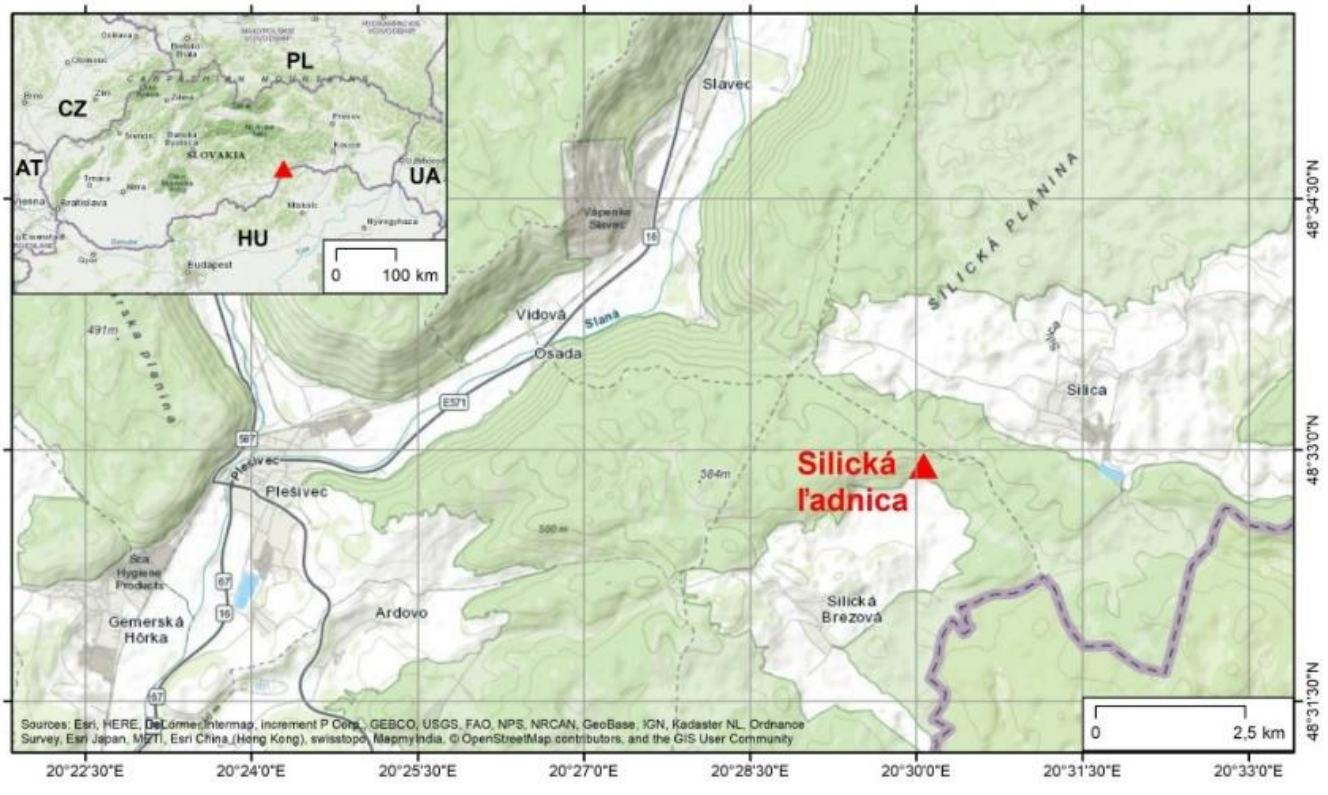

Figure 1: Location of the Silická ľadnica cave.

Over the last decades, there has been a significant decrease of the ice, which is particularly evident on the photograph (Fig. 2). Since 2014, the ice surface has been measured using total station and a map of ice distribution in the cave was produced by Ondrej (2014) (Fig. 3). As we described above, the main weaknesses of the tachymetry methods in the ice cave is the

The Cryosphere Discuss., https://doi.org/10.5194/tc-2019-82
Manuscript under review for journal The Cryosphere
Discussion started: 2 May 2019

inability to repeat measurements regularly and easily due to the hard environment. Since 2016, a novel methodological approach using laser-scanning technology focusing on monitoring a cave cryomorhology was proposed and tested.

The cave has the shape of an obliquely falling bag and can be freely accessible only from the north because of the other side form perpendicular tectonically rocky cliffs. The cave starts at the southern slope of a larger gable and the altitude of the edge of the gorge is 503 m above sea level (Bella and Zelinka, 2018) in the warm and moderate humid sub region with cold winters in January ≤−3°C and mean annual precipitation total 600–700 mm (Lapin et al., 2002, Faško and Šťastný, 2002). A light-hole corrosion-ridge is formed in light wettersteinian anise and ladine limestone, whose layers have a 30° east slope (Droppa, 1962).

Figure 2: Photographic evidence of floor environment in the Silicka ľadnica cave over last 80 years.

The bottom of the iced part of the Silicka ľadnica cave (Fig.3) is reachable from the eastern side of the debris cone, which forms fine-grained sediment and a gravel of lime blocks. The western part is covered with seasonal ice accumulations. Cave passes in lower part through a sharp edge to icefall with an average slope of 70°. Near of the lower part of the icefall is a short 20 m long passage originated by paleo-stream. At the south end of the iced area is a masked entrance to other cave parts that were discovered by J. Majko in 1931 (Stankovič and Horváth, 2004).

The Cryosphere Discuss., https://doi.org/10.5194/tc-2019-82
Manuscript under review for journal The Cryosphere
Discussion started: 2 May 2019

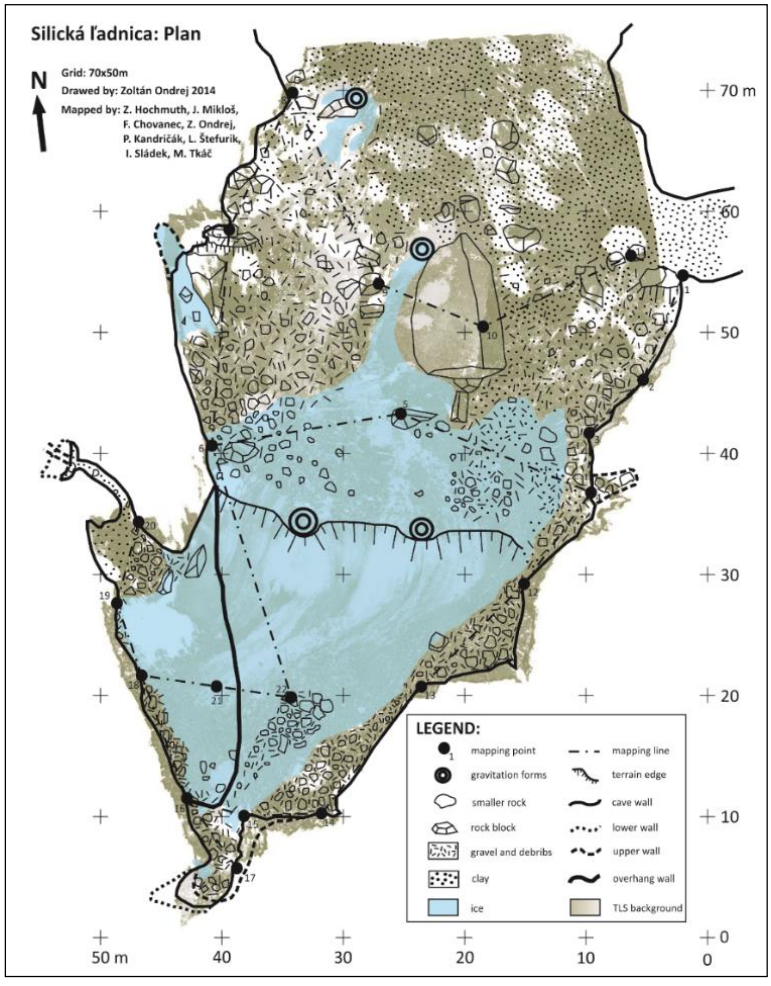

Figure 3: Plan of the cave modified according to Ondrej, 2014.

The ice accumulations in the Silická ľadnica cave has a different degree of degradation of vertical ice formations or their remains within the year. For optimal ice formation, the conditions of the slow spring warming are most appropriate, when infiltration of water from melting snow or precipitation, which then freezes in the cave. During a spring season, the thickness of emerging of the floor ice is from a few centimetres to decimetres. The thickness and area of the ice vary over the year and a large portion of the floor ice is situated beneath layers of clay, gravel and stones permanently (Stankovič and Horváth, 2004). The icefall (Fig. 4A) ends at 79 m deep in the cave (424 m above sea level) and it is unreachable to the ordinary visitors. Only few vertical gravitational ice forms are visible from the artificial sightseeing terrace accessible for visitors freely (Fig. 4B). The largest stalactite situated in central part of the cave grows up to several meters throughout spring season. There are three more mighty stalactites, two over the icefall and one in the west side of the cave near the cave entrance. The Silicka ľadnica cave comprise of manifold ice forms such as hoarfrost located mainly in the upper parts, ice

coatings on the walls of the cave, which usually appear in the lower most parts in the contact with non-iced places of the cave and others.

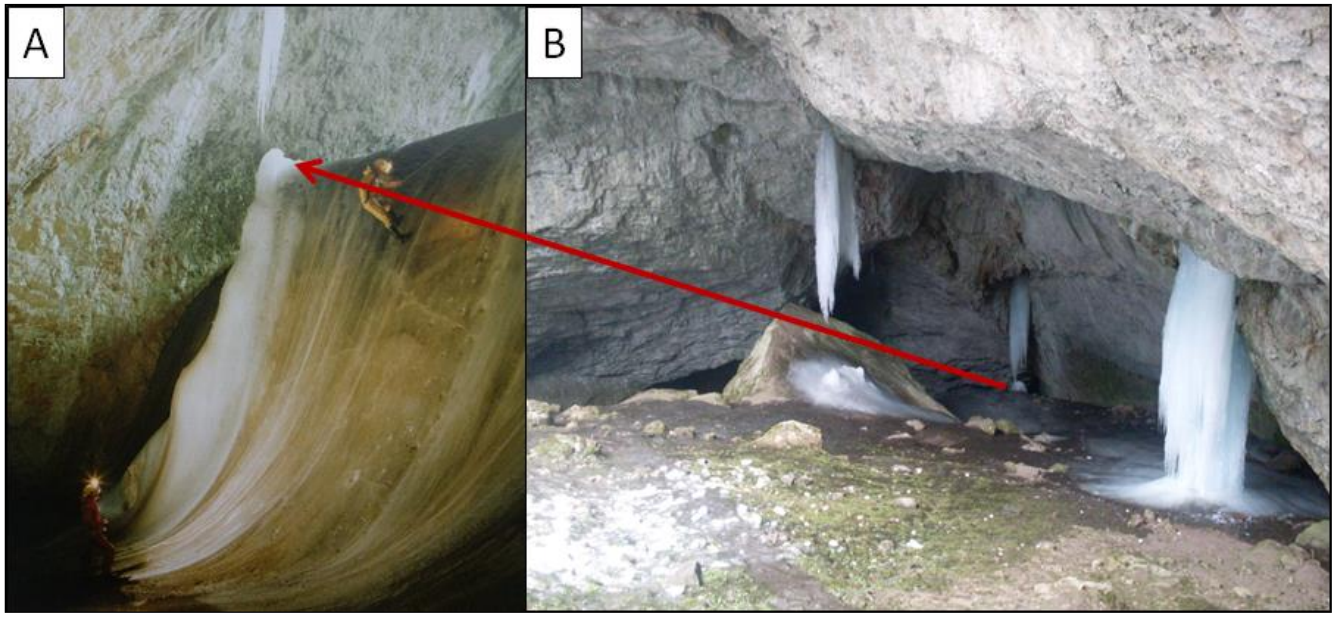

Figure 4: The Silická ľadnica cave contain different types of ice objects. The permanent ice is represented by (A) an icefall (Stankovič and Horváth, 2004) located in the bottom part of the cave. Ice speleothems (B) such as stalactites and stalagmites situated in upper part of the cave (Ondrej, 2014) are the most dynamics objects with significant seasonal changes.

The entrance of the cave was well-known for locals since ancient times. The first record with plan of the cave is dated to 1719 and it was created by Georg Buchholtz (Bella and Zelinka, 2018). In 1793, R. Townson with J. Teleki and other researchers performed the first temperature measurements (Zelinka, 2005). In this period, many locals were used the pieces of ice from the cave for a cooling of meat and beer. During the years 1863-1867, nearby the cave entrance a small brewery was built and operated (Bárta, 1995). Rajman et al. (1987) contend that this intervention related with brewery had negative consequences to the ice accumulations. E. Terlendayi performed the survey of ice surface in January 1892 and the ice was at the lowest value ever, what is similar to the range of current ice accumulations in the winter season. Other negative influence related with decrement of the cave ice correlated with change of the microclimatic situation of the cave after discovering the connection with the Archaeological Dome in 1931 by J. Majko. After opening the connection between the Archaeological Dome and the Silická Ľadnica cave lead to the inflow of warmer air from the lower non-iced area to the higher iced parts. This phenomenon is reflected in the ice melting. The long-term monitoring revealed that extent of the ice in the Silická ľadnicacave is not constant but variable in shorter periods relatively (Stankovič and Horváth, 2004).

The Cryosphere Discuss., https://doi.org/10.5194/tc-2019-82
Manuscript under review for journal The Cryosphere
Discussion started: 2 May 2019

3 Data and Methods

Data acquisition was undertaken by terrestrial laser scanner RIEGL VZ-1000.It is a full waveform pulse scanner transmitting laser beam in near infrared wavelength (1550 nm) with nominal precision of ± 8 mm at distance of 100 m and maximum scanning range up to 1400 m. Minimum scanning distance of the scanner is 1.5 m. The device dimensions are 0.3 mx 0.2 mx 0.2 m and weigh including batteries is 10 kg (Riegl 2015).

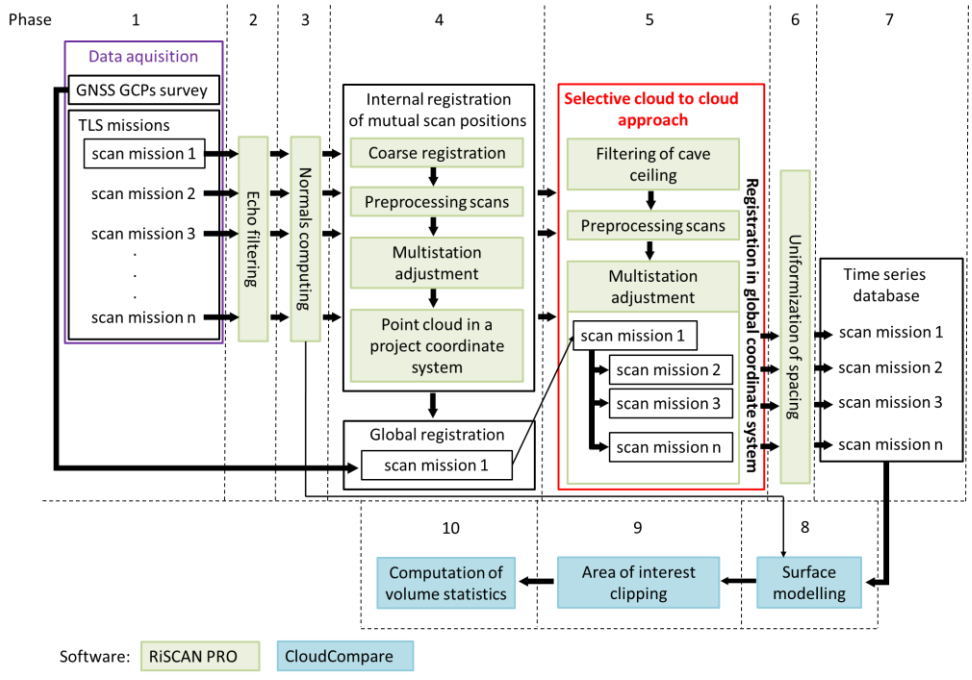

Figure 5: The workflow of generating of time series database and framework of data processing.

The parameters that allow using the scanner in ice caves despite of dimensions and weight easily. The disadvantage of using this type of scanner in caves is incomplete vertical scanning range limited to 100 degrees. This means, that it is not possible to capture a portion of view under the scanner in nadir direction and part of the ceiling above the scanner in zenith direction. The data shadows are eliminated by more frequent positions of the scanner during scanning mission. The horizontal field of vision has a range of 360 degrees.

Data collection by TLS started since June of 2016. First mapping with TLS was focusing on the testing the capability of technology to capture an ice in the cave. Until October 2018, the sixth series of scanning mission was accomplished. The number of scan positions was not unified because a placement of scan positions was determined by mainly the extend of the floor ice in the cave and (ii) sufficient overlaps eliminating shadows in final point clouds (Fig. 6).

The Cryosphere Discuss., https://doi.org/10.5194/tc-2019-82
Manuscript under review for journal The Cryosphere
Discussion started: 2 May 2019

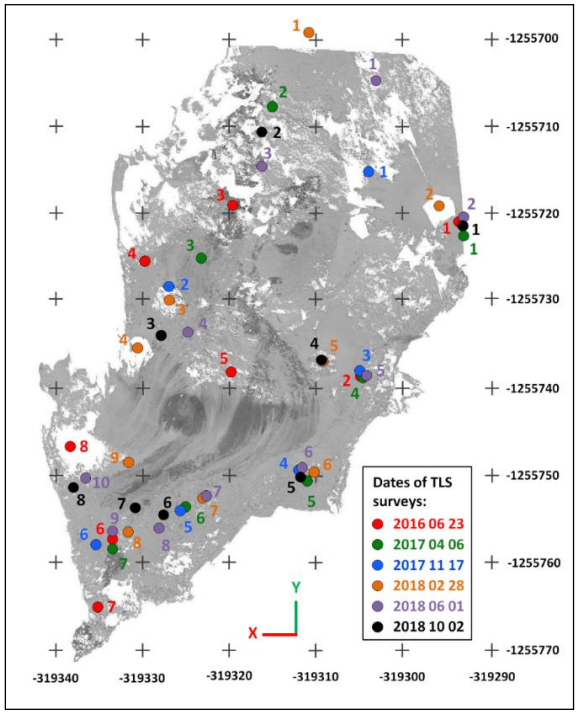

Figure 6: Distribution of scan positions of individual scan missions located within the S-JTSK (EPSG:5514) coordinate system.

The first mapping mission contains 32 individual scan positions, because of the GCPs, immediate exterior surroundings of the cave were captured as well (Fig. 5 phase 1). The scan mission 1 have used 10 GCPs for registration in global coordinate systems (Fig. 5 phase 4). All scan mission data sets are registered initial coordinate system S-JTSK (Systém jednotnej trigonometrickej siete katastrálnej – in Eng. System of the Unified Trigonometrical Cadastral Network), EPSG code 5514. The GCPs were measured by GNSS methods using the TOPCON HiPER II device with a reference connection to the Slovak observation service - SKPOS. Point measurements were performed for 30 seconds using the RTK method via weighted averaging. The coordinates of the points were calculated by TopconLink software. The standard deviation error of transformation of scan mission 1 in global coordinate system based on the GCPs is 5.3 cm.

During the scan missions, we used the settings of scanning mode Panorama 40 and Panorama 60. Using a scanning mode are enable to set some parameters of scanning detail. The Riegl VZ-1000 scanner distributes laser pulse by a rotating mirror. In the mode of Panorama 40, the scanner emits a pulse in the ambient environment every 0.04 degrees of mirror rotation in the vertical direction and 0.04 degrees in the horizontal direction. The smaller the angle, more detailed and higher the number of recordings in the resulting point cloud is captured (Tab. 1). Precision of scan mission is dependent on the number of scan positions as well. The most points were recorded within the first scan mission, where we scanned the surroundings of cave. Further scan missions have already been carried out only in the cave in the places of ice accumulations. Therefore, the number of scan positions as well as the number of points are lower compared to the first scan mission. Duration of the scanning at one position with scanner settings of range 450 metres, frequency of 300 kHz and mode of Panorama 60 takes 3

minutes and 50 seconds and with mode of Panorama 40 takes 5 minutes for 20 seconds respectively. The total scanning time of the first scan mission was approximately 12 hours due to the challenging terrain and the surrounding forest. The second time scan missions inside the cave, the scanning time did not exceed 3 hours. This time is acceptable for repeating scanning to capture the ice accumulation dynamics and generation of time series database.

Table 1: Characteristics of the time series database.

Date of survey	No. of positions	Mode of scanner (mdeg)	No. of p. after internal registration	No. of p. after uniformization of spacing and clipping AOI	St. Dev. of internal reg. (mm)	St. Dev. of global reg. (mm)
2016 06 23	32	40	476 759 981	16 408 990	3.5	Reference
2017 04 06	7	60	57 954 146	12 260 062	3.5	4.4
2017 11 17	6	60	52 148 327	11 588 910	4.1	4.2
2018 02 28	9	40	183 997 069	22 256 625	5.0	4.2
2018 06 01	10	60	81 904 050	8 798 708	4.7	4.0
2018 10 02	8	40	175 914 550	18 278 696	4.7	4.5

3.1 A framework of registration procedure using TLS data

Data processing consisted of several steps. We used the RiScan Pro software for primary data processing. After importing individual scan positions to the project, we removed the points from single scan position that are problematic for registration. In general, these are points referred to as a noise. Noise occurs during scanning in many situations. Ones of them are the impact of a laser beam on water level, or in case of false reflections in places where the laser beam traces the objects inter face. By removing the noise from point clouds of single scan positions in this phase, we improve the registration result based on automatic cloud-to-cloud approach. As noted in Gómez-Lende and Sánchez-Fernández (2018), the noise can be removed manually or automatically. In our approach, we suggest automatic noise filtration using parameters of the order of reflection and deformation of the shape of laser pulse trace. The scanner emits a laser pulse and distributes it to the ambient environment. A laser pulse has a certain shape of trace when it comes to the surface. The scanner Riegl VZ-1000 is able to record deformation of the pulse trace. This parameter is termed deviation. It is a dimensionless number with values of range 0 to 65,535. The value 0 indicates that the track has circular (ideal) shape, the value 65,535 represents the shape of the elongated ellipse of the pulse track.

The further processing, we used only points whose deviation value is in the range of 0 to 20. Thus, we filtered out less accurate measurements caused by the deformed shape of scanner pulse track. In addition, we used only points that represent the first and unique echoes. In this phase, we removed about 35-40% of the points from the point clouds of single scan positions.

The next step was to calculate the normals for points (Fig. 5 phase 3). We recommend performing this step before internal registration of mutual scan positions. The reason is that the direction of normals could be erroneously determined for cave after internal registration because of complexity of shape geometry of the cave. Derivation of normals is required for the generation of 3D model of cave surface (Fig. 5 phase 8). The direction of the normals was calculated to the scanner position. In this step, we eliminated the erroneous estimation of normals of points that could arise within methods based on calculating normals regard to the geometric centre of the point cloud as well as with determination of normals using algorithms via the analysis of neighbourhood. Finally, the normals of all points are oriented inside the cave.

After filtering the points and calculating the normals, there was a phase of internal registration of the mutual scan positions (Fig. 5 phase 4). Registration of mutual scan positions was performed within 2 steps. First, the coarse registration approach via identical points was used. The edges of the rocks on the ceiling and well-recognizable objects such as scratches were chosen as identical points. Second, the RiSCAN Pro software has an integrated multi-station adjustment (MSA) module that allows registration of mutual scan position based on cloud-to-cloud approach (Ullrich et al., 2003). This approach is built on the automatic extraction of areas defined based on certain parameters. In our case, we used a method based on filtering patches of planes. Planes were calculated at least from 5 points. Minimum search cube size was 0.128 m. Only areas whose minimum plane error was 0.02 m were used for registration of mutual scan positions. Subsequently, centroids of planes and the normals derived for them were determined. The registration of two scan positions is based on the assumption that the same areas with the same or very similar normals characteristics of planes will be identified as identical within registered scenes. The tolerance of the normals deviation is defined by the parameter of maximum tilt angle which was set to value of 1 degree. Search radius was set to value of 0.5 m. In other words, the identical planes are considered to be those that are 0.5 m far from each other and the similarity of the normal direction of their centroids are 1 deg. This way, individual scan positions were registered and a point clouds were generated and located in the local coordinate system. In order to evaluate the increase or decrease of the ice accumulations, it was necessary to place point clouds from different scan missions in a common coordinate system.

3.2 Selective cloud-to-cloud approach

We propose a selective cloud-to-cloud (sC2C) approach to register scan missions into a unified coordinate system (Fig. 5 phase 4). The proposed approach is built on identification of the stable parts of the cave, where there is no increase or decrease in mass. The first step, it is necessary to identify surfaces whose geometry is constant over a time. In the Silická ľadnica cave, the surfaces that are stable and does not change during the year due to the dynamics in the ice filling have been identified on the ceiling of the cave (Figure 7 C). These areas were extracted and used to place individual scan missions into a common coordinate system. In our case, we have located the point clouds of scan missions into the project coordinate system of scan mission one using MSA tool. Selecting the points after representing of the ceiling of the cave, we derived the planes and normals of their centroids were determined according to the same parameters as in the phase 4.

The Cryosphere Discuss., https://doi.org/10.5194/tc-2019-82
Manuscript under review for journal The Cryosphere
Discussion started: 2 May 2019

We argue that proposed sC2C approach is more suitable for automatic registration of individual scan missions because of the point cloud of the reference scan mission was locked and the propagation of errors of identical planes were distributed only at locations that we considered as stable. Thus, the residuals of normals have not been dispersed into places that could considered as similar in shape but not identical in the position. One of the problematic places for registration are stones that float on the surface of the ice and their shape does not change (Figure 7 A and B). All scan missions were placed in the S-JTSK global coordinate system because of possibility of comparison office dynamics from other older geodetic measurements.

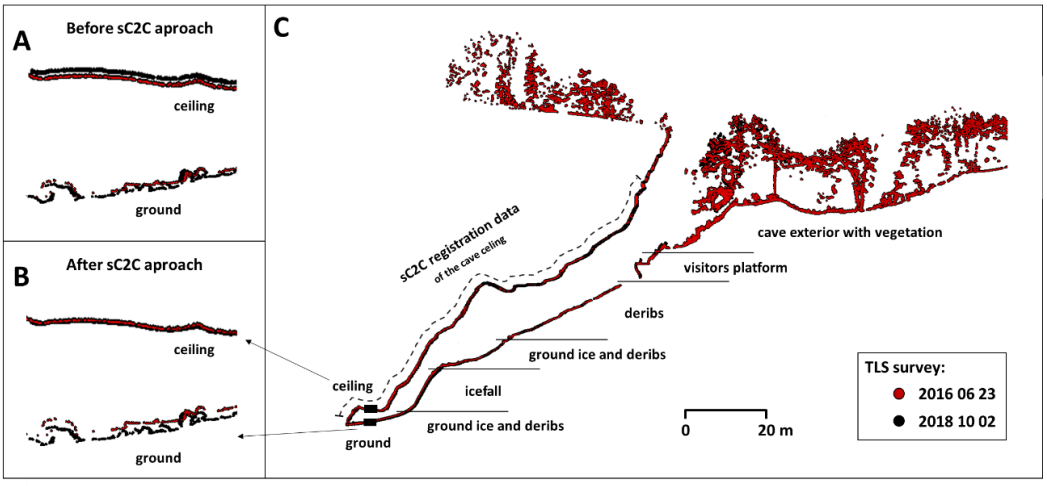

Figure 7: Result of registration of scan mission (A) before and (B) after using sC2C approach. For sC2C approach has been used stable points of the cave celling (C).

The floor ice dynamics in a cave using the TLS method can be captured with a certain degree of accuracy, which is determined by the device error ($E_{instrument}$) and the error of registering individual scan positions ($E_{registration}$). One of the advantage of the proposed sC2C method is that there is no accumulation of errors due to errors in other measurements, such as GNSS (E_{GNSS}) measurements and Global Coordinate System registration error (E_{GCS}). The total error (E_{Total}) of the proposed method can be calculated using a modified equation (1) by Collins et al. (2012):

$$E_{Total} = \sqrt{E_{instrument}{}^2 + E_{registration}{}^2} \quad (1)$$

In our case, we used the Riegl VZ-1000 for mapping, whose $E_{instrument}$ is defined by the manufacturer based on the calibration protocol and is 0.008 m. The highest standard deviation error of global registration has been reached for the measurement of 2.10.2018 and has a value of 0.0045 m. The total error E_{Total} is ± 0.0092 m, which is a threshold for recognizing the changes between measurements.

A heterogeneous distribution of points is one of the main characteristic of TLS point cloud what is resulting from (i) the methodology of data acquisition and (ii) the necessity of registration of mutual scan positions. At locations near to the

scanner position, the density of the points is higher in comparison to the farter parts from the scanner. In addition, higher density of points is mainly situated in places that are visible from multiple position, lower density of the points is located in places visible only from one position. High variability of point spatial distribution within point clouds causes problems especially for interpolation functions and modelling of derived surfaces (Gallay et al., 2016). This problem can be solved by uniformization of point spacing - the distances between points (Fig. 5 phase 6). We used 0.005 m of spacing for reduction point clouds. It leaded to decrement of 60 % of points without impact to spatial resolution of final surface model (Fig 8). Homogenization of the point distribution was performed using Octree tool implemented in RiSCAN Pro software. In the places with a lower point density is the same distribution of points in comparison with original input dataset. On other side in places with high point density (more than 7000 points per square meter) we reduced the number of points and we homogenized spatial distribution of the final point cloud. By removing redundant points, we obtained a spatially homogenized input point cloud for the calculation of cave surface models.

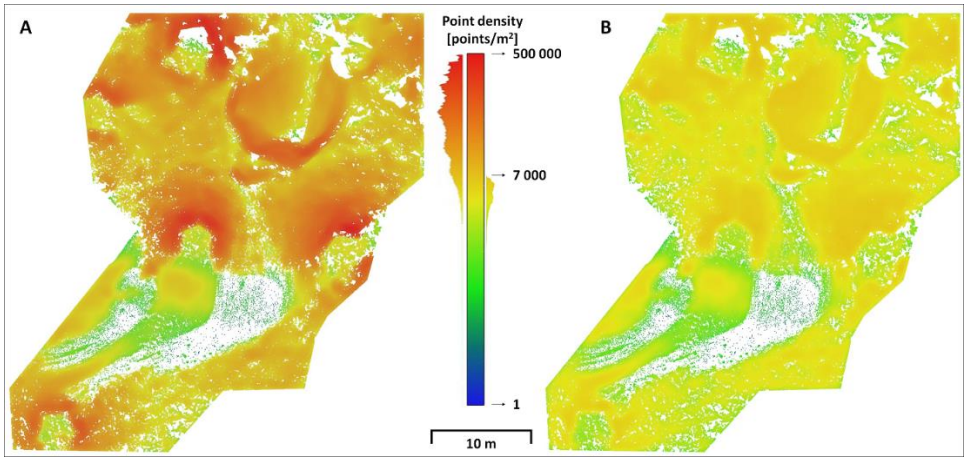

Figure 8: Distribution of point density (A) before and (B) after uniformization of spacing.

The generation of the time series from point clouds representing the ice cave is a first final product of presented paper (Fig. 5 phase 7) resulting from data collection and data processing (Fig. 5 phase 1 until phase 6). An important part of the time series creation is data management and generation of metadata.

3.3 Deriving complex 3D cave model from point clouds using mesh model

Comparison of the cave floor ice over time requires a time series of surface models derived from point clouds representing floor of the cave. The cave has a very complex geometric structure with floor, ceiling and perpendicular walls and therefore some classical bivariate functions hit to their limits and cannot be fully applied for modelling of the cave morphology. Traditionally, functions designed for modelling terrain, which general formulation is $z = f(x, y)$, are widely used. On other side, for surface modelling it is only possible to use bivariate functions, but with a local search radius (Gallay et al., 2016). The result of proposed modelling approach is a two-dimensional surface (plate) located in three-dimensional space. Thus, the

bivariate functions with general form $z = f(x, y)$ does not apply to the whole dataset but only locally e. g. for a cube with defined side length. There for, we used a vector-based mesh modelling approach to create the surface of the cave floor, which makes it possible to model such complex shapes. Ones of the key input for calculation of mesh are norms of the points that have been derived in phase 3 for each scan position individually. We used the Poisson surface reconstruction (PSR) interpolation method (Kazhdan et al., 2013) implemented in the open-source software CloudCompare (Girardeau-Montaut, 2018). The generated cave surface model by PSR is dependent on several parameters. Spatial resolution of the 3D cave surface model is controlled by Octree parameter. It is a dimensionless number used for fragmenting the space defined by the range of input data. Octree 1 means that the space of input data range is fragmented to 8 cubes, which is identical with the bounding box cube of input data. Octree 2 means that each cube from the previous step is divided into 8 smaller cubes. Thus, 64 smaller cubes are generated. In general, for calculation of the resulting fragmentation of input data range is valid the formula $8^{(\text{Octree Parameter})}$. In our case we used the value of Otree 13, where by the whole space of input data range was fragmented to 8^{13}(549.755.813.888) cubes, which represents a spatial resolution of 0.0054 m. At the respected point spacing resolution of generated point clouds (Fig. 5 phase 6) without additional generalisation of the 3D cave model. We were used a high resolution of Octree parameter, because other parameters such as samples per node and point weight did not have a significant effect on a quality of final 3D cave models. The parameter of full depth, we set the value of 8, which represents a cube with an edge size of 0.1714 m. By this parameter, the spatial resolution of triangles for parts of the 3D cave model in places with lower density of point distribution is set (Fig. 8). The lower density of point distribution is located in the icefall, where the highest point-to-point distances reaching 0.15 m. Thus, parameter of the full depth helps us to regulate and limit creation of longitudinal triangles.

Creating after the 3D cave model, it was necessary to cut the area of interest (AoI) (Fig.5 phase 9). The area of interest we considered places on the floor of the cave, where we expect the occurrence of ice. The better visualisation and understanding of ice dynamics, we have extended the polygon to the nearest surroundings. Area of AoI polygon projected orthogonally to the flat defined by x and y axes is 12,000 m^2. This step is necessary to do after 3D cave modelling (Fig. 5 phase 8), because due to the interpolation function there is deformation on the model at the border of AoI (border effect). We used a segment tool implemented in CloudCompare software to cut the models based on AoI polygon.

The resulting truncated 3D floor cave models were subtracted from each other and calculated volume changes (Fig. 5 Phase 10). To calculate volume of changes, we used the M3C2 tool (Lague et al., 2013) implemented in the CloudCompare software. Differences between 3D floor cave models within time series database were expressed by profile cartographic method (Fig. 9), gradual and inter-seasonal changes via surfaces derived from the differences of distances approach (Fig. 10) and numerically (Tab. 2).

The Cryosphere Discuss., https://doi.org/10.5194/tc-2019-82
Manuscript under review for journal The Cryosphere
Discussion started: 2 May 2019

4 Results and Discussion

Using TLS and sC2C approach leading to generation of time series database of measurements, cave floor ice dynamics could be evaluated. We decided to analyse then by two methods such as overlapping cross sections (Fig. 9) and calculating volume changes based on differences of distances using 3D floor cave models (Fig. 10). Based on the profiles of the cave floor, we can conclude that the dynamics of surface in the monitored period was significant.

4.1 Detecting cave floor ice dynamics using cross sections

All cross sections were led through identical cave sites and passed across the cave floor to represent different types of morphological structures such as stone debris, icefall, subsurface floor ice and stable elements such as large rocks attached to the subsoil structure (Fig. 9 A). A unique colour was assigned to each cross section by mapping dates (Fig. 9 B). The floor cave ice dynamics are demonstrated in selected details of cross sections showing three parts of the cave floor. The first part (Fig. 9 a) represents a foot of the icefall located in the lowest part of the cave, where a transition between the rocks connected with the subsoil structures and the stone debris with subsurface floor ice is situated.

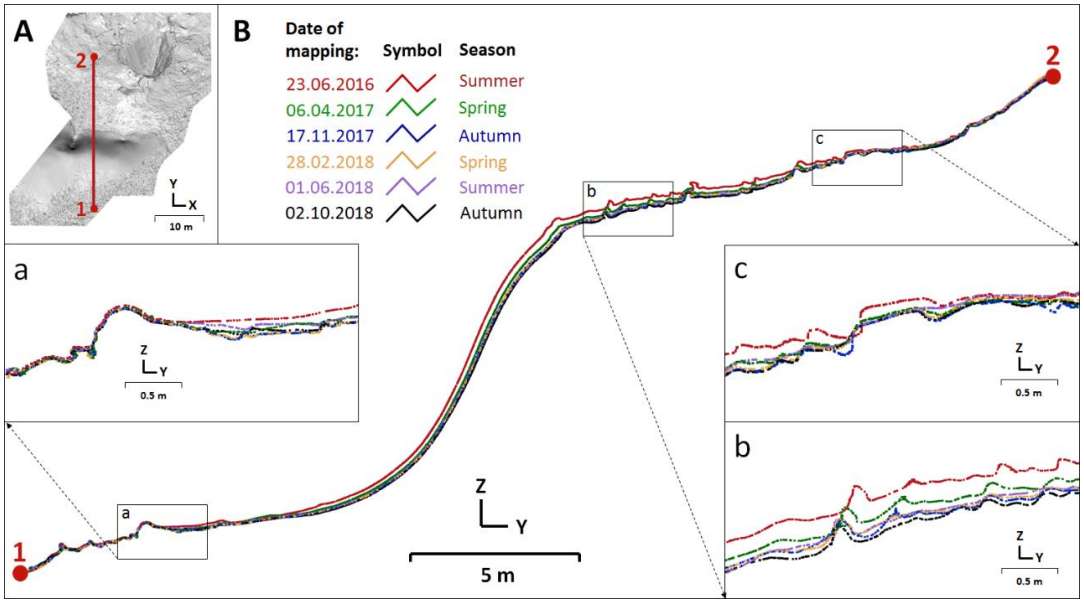

Figure 9: (A)Top view of the AoI portraying shading 3D cave floor model with the red line indicated vertical cross sections. (B) Dynamics of the cross sections representing the cave floor coloured by date of TLS survey. Details of selected parts of the cross sections representing (a) a foot of the icefall, (b) a place of the most visible dynamics of the cave floor ice and (c) the highest occurrence of the floor ice in the cave in contact with stone debris.

The second part (Fig. 9 b) shows the location with cave floor ice accumulations. On the cross section it is possible to identify rocks that seem to float on the ice surface. Their shape does not change, only their positions. The tendency of the rocks movements is in the direction of gravity to the lower parts of the cave. The third part (Fig. 9 c) there is again a stone debris passage of transitions between iced and not iced parts of the cave. A convergence of the cross sections is not as pronounced

as in a foot of the icefall (Fig. 9 a), because there is a mechanically conditional movement of the material by cavemen walk. On Fig. 9 c, it is possible to observe a random arrangement of the cross sections above a flat stone with converging character.

We argue that occurrences of cave floor ice can be identified via cross sections. The argument is based on a hypothesis that the state of ice correlates with thermal and hydrological conditions in the cave during the year and in the longer time period as well. Therefore, the ice dynamics is visible on cross sections. The locations of diverging cross sections can be regarded as the occurrences of cave floor ice, which may be under the sediment of a clastic unsorted material.

Ice dynamics is not the same in all locations. The biggest ice dynamics can be seen in the middle of the profile, which is related to the shape of the icefall. We assume that when the ice is melting, water flows into the lower parts of the icefall, where it freezes and then sublimates, or it loses in the stone debris at the bottom of the cave. In the upper parts of the profile, it can be assumed that the ice that will form in the spring, its state culminating in the beginning of the summer will melt into the autumn and will be formed again after the spring rains and creeps. The most stable state of ice is in the lowermost parts of the cave, where it is the coldest and where the dispersion of the cross sections is the smallest. It can be concluded that there was an overall decrement in ice accumulations during the reporting period.

4.2 Cave floor ice changes detected by differences of distances method

Volume changes can be better evaluated based on differences of distances method (DoD) (Fig. 10). Gradual comparison of surfaces dynamics (Fig. 10 Gradual) demonstrates that there is a constant change in ice volume. Thus, the ice in the cave constantly increases or decreases between time periods.

Between summer 2016 and spring 2017 (Fig. 10, T1-T2), ice decrement was localized mainly on the icefall, while ice increment can be seen on a big rock in the middle of the cave, where water dripping from a vertical glacier hanging from the ceiling formed ice accumulations (Fig. 4B). This phenomenon always occurs in the spring when the water from the spring rains passes through the cracks into the frozen part of the cave. A similar phenomenon can be seen in Fig. 10 T4-T5. Another phenomenon is the collapse of glacial stalactites that we caught before the autumn (Fig. 10 T3-T4). So it is not in a true sense of increment of cave ice volume, but destruction of the original glacier drops hanging from the ceiling. During the summer, ice melts and in the autumn, respectively in winter it is possible to observe a seasonal minimum in the volume of cave ice (Fig. 10 T2-T3 and Fig. 10 T5-T6).

It is interesting to study the increment of the stalagmite on the icefall (Fig. 4A), the volume of which has increased during the whole period (Fig. 10 gradual). The increment is related with a crevice in the rock ceiling, which is fulfilled with the ice stalactite. Because of the dry seasons, the stalactite has been melted and its shape was reduced. Thus, dripping water dropped to another location and a new stalagmite was formed just below.

The Cryosphere Discuss., https://doi.org/10.5194/tc-2019-82
Manuscript under review for journal The Cryosphere
Discussion started: 2 May 2019

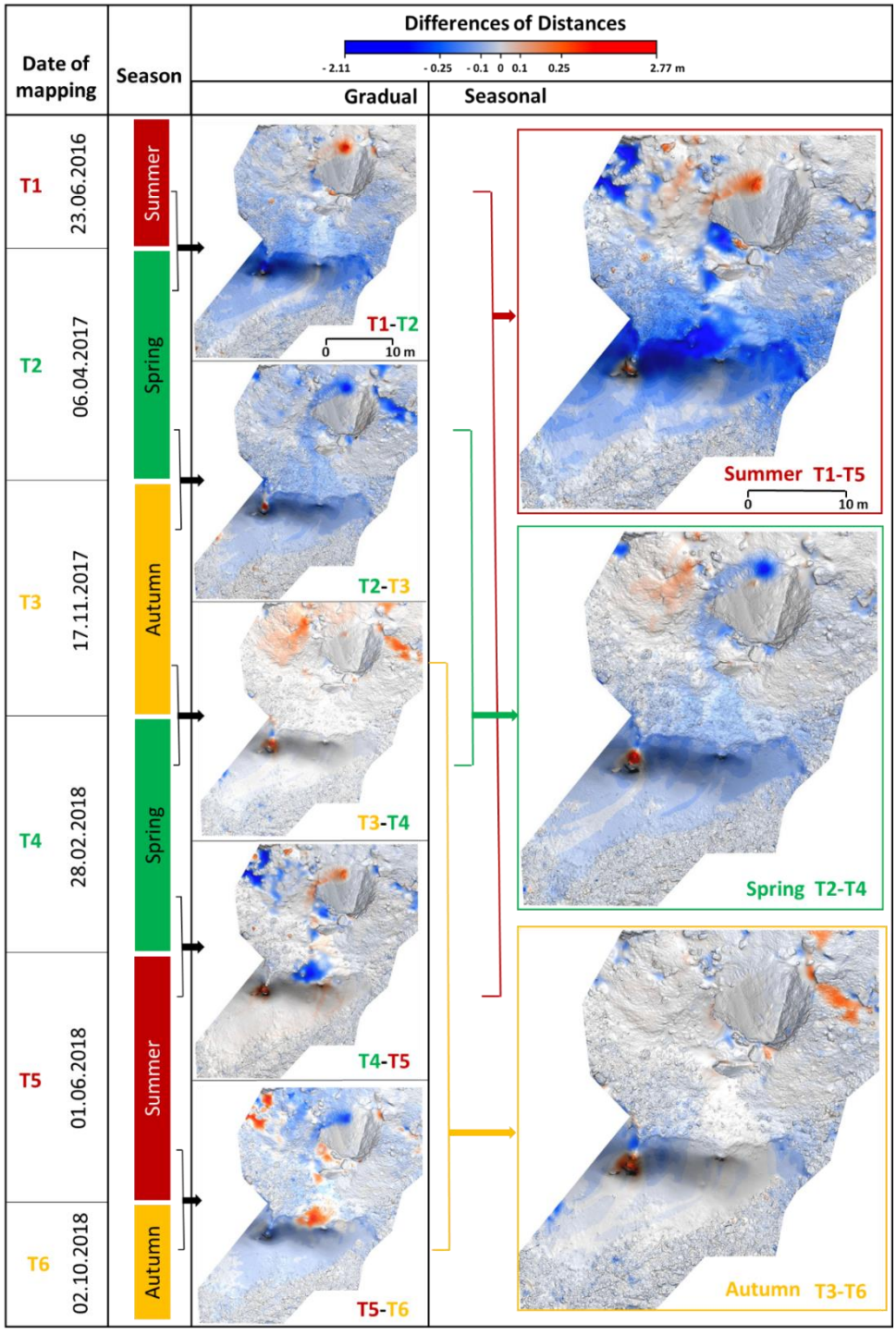

Figure 10: Differences of distances (DoD) between the individual cave floor surface models. The blue colour represents decrease and red colour indicates increase of the volume.

Naturally, the question arises as to what is causing the loss of ice accumulations in the cave and whether there is irreversible year-on-year loss of ice accumulations. To be able to qualified answer this question, it is necessary to continue in monitoring of cave ice and other factors such as temperature, precipitation as well. However, based on the presented analysis, we can conclude that the assessment of floor cave ice dynamics in terms of overall trends is only possible to observe through a season-on-season comparison between the same periods, e.g. between summer or spring seasons over a longer time period (Fig. 10 Seasonal).

A significant loss of ice accumulations has been seen in Fig. 10 T1-T5, which demonstrates the rapid decrement of ice between summer 2016 and summer 2018. DoD was calculated with respect to the z-axis, so there is a significant drop in surface, even more than 2 m. However, it should be interpreted that if the ice on a steep icefall with a slope more than 70 ° falls 0.2 m in a direction perpendicular to the slope of the profile, the difference in z-axis (height) for a place with the same x and y coordinates can reach 2 m, which is visible from the comparison of individual cross sections (Fig. 9 B and Table 2 Max. Decrease).

The red colour shows the increment in two places, which were demonstrated in Fig. 4. The increment in the massive rock in the middle of the cave was caused by the destruction of the glacial stalactite. The second distinctive height increment is located on the icefall in the form of stalagmite, which is formed from dripping water from the shrinking stalactite hanging from the crevice in the cave ceiling, as described above. Another inter-seasonal comparison between spring 2017 and spring 2018 (Fig. 10 T2-T4) indicates a year-on-year loss of ice. In the case of DoD between autumn 2017 and autumn 2018 (Fig. 10 T3-T6), there is no significant decrement or increment of ice accumulations. We can conclude that the ice volume is comparable between these periods, so, it is stabilized.

The biggest benefit of the created time series database of complex 3D surface model is also in the quantification of the volume changes of the cave floor ice and its expression through summary numerical statistics (Table 2).

Table 2: Summary statistics of volumetric and vertical changes of the selected cave floor extent during the monitored period.

Differences of distances (DoD)	Type	Total vol. change [m^3]	Increment of volume [m^3]	Decrement of volume [m^3]	Avg. change of surface [m]	Max. increase [m]	Max. decrease [m]
T1-T2	gradual	-73.20	13.76	86.96	-0.060	1.20	1.59
T2-T3	gradual	-67.03	07.18	74.21	-0.054	2.52	1.38
T3-T4	gradual	32.35	41.57	09.22	0.027	1.30	0.96
T4-T5	gradual	05.70	32.75	27.04	0.003	2.14	0.89
T5-T6	gradual	-42.85	16.46	59.31	-0.031	2.77	2.11
Summer T1-T5	seasonal	-102.13	15.17	117.31	-0.085	1.34	0.89
Spring T2-T4	seasonal	-34.69	16.68	51.37	-0.028	1.75	1.33
Autumn T3-T6	seasonal	-04.68	20.51	25.19	-0.001	2.50	1.33

Given the total error of E_{Total} 0.0092 m and the area of observation of 1,200 m^2, it should be emphasized that a volume of up to 10.04 m^3 may be the result of a measurement error. The highest difference in ice volume was observed at the beginning of the monitored period between summer of 2016 and spring of 2017 (Fig. 10 T1-T2) and spring of 2017 and autumn of 2017 (Fig. 10 T2-T3), when a total ice loss was approximately 70 m^3 in both cases (Tab. 2). Significant loss of ice in these periods can also be identified from the average change of surface, which in this period reaches a loss of about 0.06 m. The highest increase was recorded between autumn of 2017 and spring of 2018, when new ice from spring rains is usually formed in the cave. The increase in ice should culminate in summer, but in 2018 there was little rainfall and relatively warm. Thus, during the spring and summer of 2018, the new ice did not form. The loss of ice between summer and autumn of 2018 is already a natural phenomenon. The inter-seasonal comparison suggests that there is a significant loss of ice due to the lack of water flowing into the cave during the monitored period, as evidenced by the comparison between the summer of 2016 and the summer of 2018, when about 100 m^3 of ice were lost in the cave.

5 Conclusions

Ice caves can be considered as an indicator of the long-term changes in the landscape. Hydrological and climatic dynamics of the landscape are manifested in the ice caves and it is well-recognizable because of the caves are evidently linked with immediate surroundings. The interpretation of the dynamics in the ice cave accumulations is a challenging task that should be based on long-term and regular monitoring. In the paper we presented the analysis of the floor ice dynamics in the Silická ľadnica cave.

We used terrestrial laser scanning to map dynamics of cave sediments containing ice accumulations. In order to evaluate the changes in the cave ice accumulations, it was necessary to register the individual mappings into a uniform coordinate system. For this purpose, we have proposed an innovative method based on automatic registration of the individual scan positions using stable objects of the cave such the ceiling of the cave. The presented selective cloud-to-cloud approach brings several advantages. Using the sC2C approach, the mapping time is a shortening because it is not necessary to map the exterior surroundings of cave within repeating scan missions because of GCPs. This approach also reduces the overall registration error to the unified coordinate system as it eliminates measurement errors through GNSS. Finally, proposed framework of data processing unable to generate a time series 3D database of interior cave surface at high-scale resolution. We also presented a procedure for the modelling of complex 3D surfaces from point clouds. Presented data and the methods serve us to evaluate the dynamics of the cave floor ice. Cave floor ice dynamics has been detected based on cross sections method and via differences of distances analysis. Complex 3D models of cave floor have also been used to quantify the volume changes which we have expressed numerically.

The presented results show that there was a significant loss of ice in the cave during the monitored period. Temperature monitoring is also carried out in the cave and rainfall stations are located around the cave. Results from these monitoring

stations were not included into the presented paper. However, based on our observation as well as presented analysis of the cave floor ice dynamics, we can conclude that the loss of ice is not related with warming climate but with extremely dry years. In the presented paper, we focused mainly on the presenting the methodological approach of the high-detailed mapping of the cave ice accumulations, data processing and generation of time series database. We argue that the presented methodological framework of sC2C approach has potential to be used in other applications where it is necessary to identify landscape dynamics, such as mountain glacier assessment and sediment accumulation dynamics analysis.

Acknowledgement

With support by grants VEGA 1/0963/17: Landscape dynamics in high resolution, APVV-15-0054: Physically based segmentation of geodata and its geoscience applications, VEGA 1/0839/18 Development of a new v3.sun module designed for calculation of the solar energy distribution for digital geodata derived from a point cloud using adaptive triangulation methods.

References

Avian, M. and Bauer, A.: First results on monitoring glacier dynamics with the aid of Terrestrial Laser Scanning on Pasterze Glacier (Hohe Tauern, Austria), Grazer Schriften der Geographie und Raumforschung, 41, 27-36, 2006.

Avian, M., Kellerer-Pirklbauer, A., and Lieb, G.: Geomorphic consequences of rapid deglaciation at Pasterze glacier, Hohe Tauern range, Austria, between 2010 and 2013 based on repeated terrestrial laser scanning data, Geomorphology, 310, 1-14, doi:10.1016/j.geomorph.2018.02.003, 2018.

Barnhart, B.T. and Crosby, T.B.: Comparing Two Methods of Surface Change Detection on an Evolving Thermokarst Using High-Temporal-Frequency Terrestrial Laser Scanning, Selawik River, Alaska, Remote Sens., 5, 6, 2813-2837, doi:10.3390/rs5062813, 2013.

Bárta, J.: Pomoc archeológie pri datovaní zaľadnenia Silickej ľadnice [Archeology assistence at the dating of glaciation of the Silická ľadnica Cave], in: Ochrana ľadových jaskýň, edited by: Bella, P., Dobšinská Ľadová Jaskyňa, 21.–22. 9. 1995, SSJ, Liptovský Mikuláš, 81-84, 1995.

Bauer, A., Paar, G., and Kaufmann, V.: Terrestrial laser scanning for rock glacier monitoring, in: Permafrost, edited by: Phillips, M., Springman, S.M., Arenson, L.U., Taylor and Francis, London, 55-60, 2003.

Bella, P. and Zelinka, J.: Chapter 29 - Ice Caves in Slovakia, in: Ice Caves, edited by: Perșoiu, A., Lauritzen, S. E., Elsevier, 657-689, doi:10.1016/B978-0-12-811739-2.00029-2, 2018.

Buchroithner, M.F., Milius, J., and Petters, C.: 3D Surveying and visualisation of the biggest ice Cave on Earth, in: Proceedings 25th International Cartographic Conference, Paris, France, 3-8 July 2011.

Buchroithner, M.F., Petters, C., and Pradhan, B.: Three-dimensional visualisation of the worldclass-prehistoric site of the Niah Great Cave, Borneo, Malaysia, in: Interdisciplinar Conference on Digital Cultural Heritage, edited by: Kremens, H., Saint-Dié-des-Vosges, 2-4 July, 2012.

Collins, B., Corbett, S., Fairly, H., Minasian, D., Kayen, R., Dealy, T., and Bedford, D.: Topographic Change Detection at Select Archeological Sites in Grand Canyon National Park, Arizona, 2007–2010: US Geologic Survey Scientific Investigation Report 2012–5133, 77 pp., 2012.

Cosso, T., Ferrando, I., and Orlando, A.: Surveying and mapping a cave using 3D laser scanner: the open challenge with free and open source software, Int. Arch. Photogramm. Remote Sens. Spatial Inf. Sci., XL-5, 181-186, doi:10.5194/isprsarchives-XL-5-181-2014, 2014.

Deems, J., Painter, T., and Finnegan, D.: LiDAR measurement of snow depth: a review, Journal of Glaciology, 215, 467-479, doi:10.3189/2013JoG12J154, 2013.

De Waele, J., Fabbri, S., Santagata, T., Chiarini, V., Columbu, A., and Pisani, L.: Geomorphological and speleogenetical observations using terrestrial laser scanning and 3D photogrammetry in a gypsum cave (Emilia Romagna, N. Italy), Geomorphology, 319, 47-61, doi:10.1016/j.geomorph.2018.07.012, 2018.

Droppa, A.: Gombasecká jaskyňa [Gombasecká cave], Šport, Bratislava. 115 pp., 1962.

Fabbri, S., Sauro, F., Santagata, T., Rossi, G., and De Waele, J.: High-resolution 3-D mapping using terrestrial laser scanning as a tool for geomorphological and speleogenetical studies in caves: An example from the Lessini mountains (North Italy), Geomorphology, 280, 16-29, doi:10.1016/j.geomorph.2016.12.001, 2017.

Faško, P. and Šťastný, P.: Mean annual precipitation totals, in: Landscape Atlas of the Slovak Republic, Ministry of Environment of the Slovak Republic, Bratislava / Slovak Environmental Agency, Banská Bystrica, Map No. 54, p. 99, 2002.

Fischer, M., Huss, M., Kummert, M., and Hoelzle, M.: Application and validation of long-range terrestrial laser scanning to monitor the mass balance of very small glaciers in the Swiss Alps, The Cryosphere, 10, 1279-1295, doi:10.5194/tc-10-1279-2016, 2016.

Fuhrmann, K.: Monitoring the disappearance of a perennial ice deposit in Merrill Cave, Journal of Cave and Karst Studies, 69, 256-265, 2007.

Gabbud, C., Micheletti, N., and Lane, S.N.: Lidar measurement of surface melt for a temperate Alpine glacier at the seasonal and hourly scales, Journal of Glaciology, 229, 963-974, doi:10.3189/2015JoG14J226, 2015.

Gallay, M., Kaňuk, J., Hochmuth, Z., Meneely, J., Hofierka, J., and Sedlák, V.: Large-scale and high-resolution 3-D cave mapping by terrestrial laser scanning: a case study of the Domica Cave, Slovakia, International Journal of Speleology, 44, 277-291, doi:10.5038/1827-806X.44.3.6, 2015.

Gallay, M., Hochmuth, Z., Kaňuk, J., and Hofierka, J.: Geomorphometric analysis of cave ceiling channels mapped with 3-D terrestrial laser scanning, Hydrology and Earth System Sciences, 20, 5, 1827-1849, doi:10.5194/hess-20-1827-2016, 2016.

Gašinec, J., Gašincová, S., Černota, P., and Staňková, H.: Uses of Terrestrial Laser Sanning in Monitoring of Ground Ice within Dobšinská Ice Cave, Journal of the Polish Mineral Engineering Society, 30, 31-42, 2012.

Gašinec, J., Gašincová, S., Zelizňaková, V., Palková, J., and Kuzevičová, Ž.: Analysis of Geodetic Network Established Inside the Dobšinská Ice Cave Space / Analýza Geodetickej Siete Zriadenej V Priestoroch Dobšinskej Ľadovej Jaskyne, GeoScience Engineering, 60, 45-54, doi:10.2478/gse-2014-0005, 2014.

Girardeau-Montaut, D.: CloudCompare - 3D point cloud and mesh processing software. Open Source Project, https://www.danielgm.net/cc/, 2018.

Gómez-Lende, M. and Sánchez-Fernández, M.: Cryomorphological Topographies in the Study of Ice Caves, Geosciences, 8, 250-274, doi:10.3390/geosciences8080274, 2018.

Gonzalez-Aguilera, D., Muoz, A.L., Lahoz, J.G., Herrero, J.S., Corchon, M.S., and Garcia, E.: Recording and modeling Paleolithic caves through laser scanning, in: Proceedings of International Conference on Advanced Geographic Information Systems & Web Services, Cancun, 19-26, 2009.

Hoffmeister, D., Zellmann, S., Kindermann, K., Pastoors, A., Lang, U., Bubenzer, O., Weniger, G.C., and Bareth, G.: Geoarchaeological site documentation and analysis of 3D data derived by terrestrial laser scanning, ISPRS Ann. Photogramm. Remote Sens. Spatial Inf. Sci., II-5, 173-179, doi:10.5194/isprsannals-II-5-173-2014, 2014.

Idrees, M.O. and Pradhan, B.: 2016 – A decade of modern cave surveying with terrestrial laser scanning: A review of sensors, method and application development, International Journal of Speleology, 45, 71-88, doi:10.5038/1827-806X.45.1.1923, 2016.

Jörg, P., Fromm, R., Sailer, R., and Schaffhauser, A.: Measuring snow depth with a terrestrial laser ranging system, in: Proceedings of the 2006 International Snow Science Workshop, Telluride, Colorado, 452-460, 2006.

Kamintzis, J., Jones, P.P.J., Irvine-Fynn, T., Holt, O., Bunting, P., Jennings, S., Porter, P.R., and Hubbard, B.: Assessing the applicability of terrestrial laser scanning for mapping englacial conduits, Journal of Glaciology, 243, 1-12, doi:10.1017/jog.2017.81, 2018.

Kaasalainen, S., Kaartinen, H., and Kukko, A.: Snow cover change detection with laser scanning range and brightness measurements, EARSeL eProceedings, 7, 133-141, 2008.

Kazhdan, M. and Hoppe, H.: Screened Poisson surface reconstruction, ACM Trans. Graph. 32, 3, Article 29, doi:10.1145/2487228.2487237, 2013.

Kern, Z. and Perșoiu, A.: Cave ice–the imminent loss of untapped mid-latitude cryospheric palaeoenvironmental archives, Quaternary Science Reviews, 67, 1-7, doi:10.1016/j.quascirev.2013.01.008, 2013.

Kern, Z. and Thomas, S.: Ice level changes from seasonal to decadal time-scales observed in lava tubes, lava beds national monument, NE California, USA, Geogr. Fis. Din. Quat., 37, 151-162, doi:10.4461/GFDQ.2014.37.14, 2014.

Lague, D., Brodu, N., and Leroux, J.: Accurate 3D comparison of complex topography with terrestrial laser scanner: Application to the Rangitikei canyon (N-Z), ISPRS Journal of Photogrammetry and Remote Sensing, 82, 10-26, doi:10.1016/j.isprsjprs.2013.04.009, 2013.

Lapin, M., Faško, P., Melo, M., Šťastný, P., and Tomain, J.: Climatic regions, in: Landscape Atlas of the Slovak Republic, Ministry of Environment of the Slovak Republic, Bratislava / Slovak Environmental Agency, Banská Bystrica, map No. 27, p. 95, 2002.

Lerma, L.J., Navarro, S., Cabrelles, M., and Villaverde, V.: Terrestrial laser scanning and close range photogrammetry for 3D archaeological documentation: the Upper Palaeolithic Cave of Parpalló as a case study, Journal of Archaeological Science, 37, 3, 499-507, doi:10.1016/j.jas.2009.10.011, 2010.

Luetscher, M., Bolius, D., Schwikowski, M., Schotterer, U., and Smart, P.L.: Comparison of techniques for dating of subsurface ice from Monlesi ice cave, Switzerland, Journal of Glaciology, 53, 374-384, doi:10.3189/002214307783258503, 2007.

May, B., Spötl, C., Wagenbach, D., Dublyansky, Y., and Liebl, J.: First investigations of an ice core from Eisriesenwelt cave (Austria), The Cryosphere, 5, 81-93, doi:10.5194/tc-5-81-2011, 2011.

Ondrej, Z.: Mikroklíma Silickej ľadnice a jej vplyv na zmeny ľadovej výplne [Microclimate of the Silická ľadnica cave and its influence on changes in ice filling], Diploma thesis, Univerzita P.J. Šafárika v Košiciach PF UPJŠ ÚGE, 91 pp., 2014.

Perșoiu, A. and Pazdur, A.: Ice genesis and its long-term mass balance and dynamics in Scărisoara Ice Cave, Romania, The Cryosphere 5, 45-53, doi:10.5194/tc-5-45-2011, 2011.

Perșoiu, A.: Chapter 4.3 - Ice Dynamics in Caves, in: Ice Caves, edited by: Perșoiu, A., Lauritzen, S. E., Elsevier, 97-108, doi:10.1016/B978-0-12-811739-2.00034-6, 2018.

Perșoiu, A. and Lauritzen, S.E.: Ice Caves, Elsevier, p. 752, doi:10.1016/C2016-0-01961-7, 2018.

Pflitsch, A., Schörghofer, N., Smith, S.M., and Holmgren, D.: Massive Ice Loss from the Mauna Loa Icecave, Hawaii, Arctic, Antarctic, and Alpine Research, 48, 33-43, doi:10.1657/AAAR0014-095, 2016.

Prokop, A.: Assessing the applicability of terrestrial laser scanning for spatial snow depth measurements, Cold Reg. Sci. Technol., 54, 155-163, doi:10.1016/j.coldregions.2008.07.002, 2008.

Rajman, L., Roda, Š., Roda Jr., Š., and Ščuka, J.: Termodynamický režim Silickej ľadnice [Thermodynamic regime of the Silická ľadnica Cave], Slovenský kras 25, 29–63, 1987.

Riegl Laser Measurement Systems GmbH, Austria: 3D Terrestrial laser scanner Riegl VZ-400 / Riegl VZ-1000 / Riegl VZ-2000 General Description and Data Interfaces, 2015.

Rüther, H., Chazan, M., Schroeder, R., Neeser, R., Held, C., Walker, J.S., Matmon, A., and Horwitz, K.L.: Laser scanning for conservation and research of African cultural heritage sites: the case study of Wonderwerk Cave, South Africa, Journal of Archaeological Science, 36, 9, 1847-1856, doi:10.1016/j.jas.2009.04.012, 2009.

Silvestre, I., Rodrigues, I.J., Figueiredo, M., and Veiga-Pires, C.: High-resolution digital 3D models of Algar do Penico Chamber:limitations, challenges, and potential, International Journal of Speleology, 44, 1, 25-35, doi:10.5038/1827-806X.44.1.3, 2014.

Stankovič, J. and Horváth, P.: Jaskyne Slovenského krasu v živote Viliama Rozložníka [Caves of the Slovak karst in live of Viliam Rozložnik], Speleoklub Minotaurus, Rožňava, 190 pp., 2004.

Ullrich, A., Schwarz, R., and Kager, H.: Using hybrid multi-station adjustment for an integrated camera laser-scanner system, Optical 3-D Measurement Techniques IV, 1, 298-305, 2003.

Vosselman, G. and Maas, H.G.: Airborne and terrestrial laser scanning, Whittles Publishing, Dunbeath, p. 318, 2010.

Xu, C., Li, Z., Li, H., Wang, F., and Zhou, P.: Long-range terrestrial laser scanning measurements of summer and annual mass balances for Urumqi Glacier No. 1, eastern Tien Shan, China, The Cryosphere Discuss., doi:10.5194/tc-2018-128, in review, 2018.

Zelinka, J.: Klíma krasových území a jaskýň [Climate of karst territories and caves], in: Jaskyne svetového dedičstva na Slovensku, edited by: Jakál, J., L. Mikuláš (Slovak caves administration), 77-86, 2005.